doi: 10.15407/ujpe62.02.0106

V.N. UVAROV,[1] N.V. UVAROV,[1] S.A. BESPALOV,[2] M.V. NEMOSHKALENKO [1]

[1] G.V. Kurdyumov Institute for Metal Physics, Nat. Acad. of Sci. of Ukraine
(36 Vernadskyi Ave., Kyiv 03142, Ukraine; e-mail: uvarov@imp.kiev.ua)
[2] Presidium of the NAS of Ukraine
(54 Volodymyrs'ka Str., Kyiv 01601, Ukraine)

PACS 31.15.-p, 71.15.Mb, 71.30.+h, 78.70.En, 72.60.+g

ATOMIC DISORDERING AND ELECTRON BAND STRUCTURE IN THE HEUSLER ALLOY CoTiSb

With the help of the Linearized Augmented Plane Wave (LAPW) method, the role of some structural types of CoTiSb alloy in the formation of its energy, spatial, spectral, and spin characteristics has been clarified. The ground state of CoTiSb alloy, which is characterized by the highest cohesive energy, is found to be realized in the case where atoms and vacancies are arranged like in the $C1b^a$ phase. Transitions to the $L2_c^a$ and $B2^c$ phases with different arrangements of alloy components in their crystal lattices are accompanied by the emergence of high-energy metastable states. CoTiSb alloy in the ground state is a nonmagnetic insulator. The metastable phases transform into metals with spin-polarized electron states and magnetic moments mainly localized at cobalt atoms.

K e y w o r d s: band structure calculations, X-ray electron spectra, spintronics.

1. Introduction

CoTiSb alloy was first synthesized in work [1]. At present, it is a classical representative of half-Heusler compounds, which are characterized by a certain combination of magnetic, transport, optical, magnetooptical, superconducting, and other important properties. With the help of those compounds, the topologic insulators and the so-called half-metallic state of a solid can be implemented. The latter has an uncompensated spin density of band electrons at the Fermi level, which is an important property required in technologies aimed at the creation of materials for spintronics. The cubic modification is the most typical of them. This modification is most often imagined in the form of four face-centered crystal lattices penetrating one another. The composition of those alloys is predominantly described by the formula VABC, where V stands for an atomic vacancy, A and B are metals, and C is a nonmetal.

A bright feature of the Heusler phases consists in the capability for their composition components to migrate over all four mentioned fcc sublattices, which substantially manifests itself in the Heusler phase properties [2]. This migration is described by arbitrary values for the occupation numbers of the sites in those sublattices with respect to the components of indicated alloys. Evidently, this circumstance will result in the infinite number of structural types characterized by different combinations in the arrangement of atoms and vacancies. However, if the allowed occupation numbers are confined to the set $\left(0, \frac{1}{2}, 1\right)$, forty-two independent structural types can be formed in the cubic modification of half-Hausler alloys. Mathematically, they are defined by the corresponding matrices of population parameters (see below) for the sites in the crystal sublattices under discussion [3]. According to the conclusions of work [3], information about

those matrices can be obtained from diffraction measurements.

Some problems concerning interrelations between atomic disorderings and the properties of half-Heusler alloys were considered in a number of works (see, e.g., works [2, 4–7]). However, those publications contain only scarce information on CoTiSb alloy. In particular, some mutual exchanges of atoms transform the alloy from the semimetallic (this is obviously a false statement, at least for temperatures exceeding 113 K [8, 9]) non-magnetic state into the metallic one [4]. The statement about the influence of possible atomic disordering on the resistive and thermoelectric properties of this alloy subjected to various conditions of a thermal treatment [7] also turned out poorly substantiated.

Therefore, in that work, where band structure calculations were mainly used, a separate model problem was considered. It concerns the role of some atomic disorderings (structural types) in CoTiSb alloy in the formation of the energy, spatial, spectral, and spin characteristics of this compound.

2. Calculation Procedure

In this work, we will calculate the electron band structures for CoTiSb alloy in its three structural modifications. The modifications differ from one another by the arrangement of atoms and vacancies in the crystal lattice. Each modification corresponds to a definite structural type. Each type is defined in the general form by means of a matrix of occupation numbers for four fcc sublattices (α, β, γ, δ), which mutually penetrate one another (Fig. 1) [3]:

$$\left\| \begin{matrix} \alpha_V & \alpha_A & \alpha_B & \alpha_C \\ \beta_V & \beta_A & \beta_B & \beta_C \\ \gamma_V & \gamma_A & \gamma_B & \gamma_C \\ \delta_V & \delta_A & \delta_B & \delta_C \end{matrix} \right\|.$$

Here, for example, the quantity γ_B means the probability of population (the occupation number) of the γ-sublattice by component B, and δ_V the site population in the δ-sublattice by vacancies V. In our specific case of CoTiSb alloy, the components are vacancies (component V), Co (component A), Ti (component B), and Sb (component C). Three structural types (phases, modifications) defined by the matrices of occupation numbers [3] were chosen for calculations, namely:

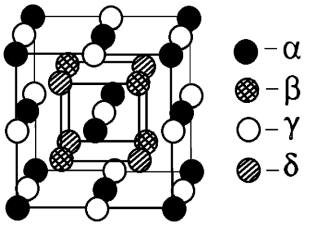

Fig. 1. Unit cell formed by four fcc sublattices (α, β, γ, δ) that mutually penetrate one another [3]

$$\begin{matrix} \mathrm{C1b}^a \\ \left\| \begin{matrix} 1 & 0 & 0 & 0 \\ 0 & 0 & 1 & 0 \\ 0 & 1 & 0 & 0 \\ 0 & 0 & 0 & 1 \end{matrix} \right\| \end{matrix} \quad \begin{matrix} \mathrm{L2}_1^a \\ \left\| \begin{matrix} \frac{1}{2} & \frac{1}{2} & 0 & 0 \\ 0 & 0 & 1 & 0 \\ \frac{1}{2} & \frac{1}{2} & 0 & 0 \\ 0 & 0 & 0 & 1 \end{matrix} \right\| \end{matrix} \quad \begin{matrix} \mathrm{B2}^c \\ \left\| \begin{matrix} \frac{1}{2} & 0 & 0 & \frac{1}{2} \\ 0 & \frac{1}{2} & \frac{1}{2} & 0 \\ \frac{1}{2} & 0 & 0 & \frac{1}{2} \\ 0 & \frac{1}{2} & \frac{1}{2} & 0 \end{matrix} \right\| \end{matrix}.$$

The values of structure-amplitude factors, which were calculated on the basis of those matrices, can be compared with their corresponding values that are determined from diffraction data. In such a way, we can establish which of the CoTiSb alloy phases is realized in the synthesized specimens with the highest probability. It turned out [3] that, in the case of CoTiSb alloy, the $\mathrm{C1b}^a$ phase is realized with the highest probability, whereas the formation of the ${\mathrm{L2}_1}^a$ structure has a low probability. The highest probability for the structure-amplitude factor of the $\mathrm{B2}^c$ phase is that it does not to correspond to experimental observations, which means that the researched alloy cannot exist in the $\mathrm{B2}^c$ modification.

In this work, in order to simplify the calculation procedure for the examined phases, the positions of alloy components were assigned by means of their multiplication, by using the symmetry operations for a simple cubic lattice P. Note that in the framework of the standard group-theory approach to the classification of crystalline solids, the arrangement of atoms in the $\mathrm{C1b}^a$ phase in the symmetry of P lattice corresponds to the cubic system with the space group F-43m (No. 216) [9]. In this work, this coincidence was used as one of the criteria of that the procedure selected for the calculation of the electron band structure in the analyzed phases with the use of P lattice is correct.

The band structure calculations were performed, by using the Linearized Augmented Plane Wave (LAPW) method [10] with the generalized gradient

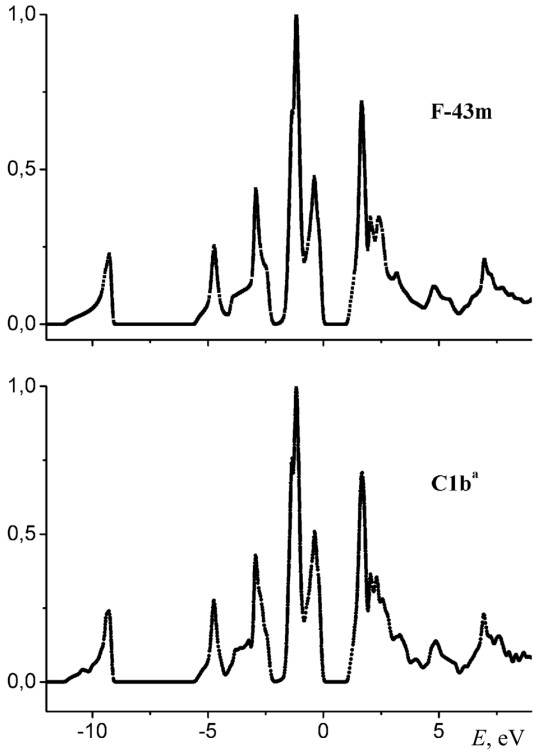

Fig. 2. Total electron densities of states in CoTiSb alloy in its F-43m and C1b^a modifications normalized to the height of the corresponding main maximum. Zero energy values correspond to the Fermi level position

approximation (GDA) of the electron density (see work [11]). While calculating the parameters of the electron band structure, a spin-polarized variant of this method was applied [12]. There is no information in the literature concerning the values of the parameter a for the cubic lattices in the $L2_1{}^a$ and B2^c modifications. Therefore, they were calculated by minimizing the total energy of the CoTiSb alloy spatial structure [12]. In so doing, the data obtained experimentally [9] for the F-43m configuration, which was optimized together with the structure of the alloy concerned in the C1b^a modification (it was done to implement the same approach in calculations), were taken as the initial values for the.parameter a.

Optimized values of the parameter a for a unit cell in various structural types of CoTiSb compound

Structural type	F-43m	C1b^a	$L2_1{}^a$	B2^c
a, Å	5.8934 5.8825 *	5.8907	5.9343	6.2123

* Experiment [9].

The results obtained are quoted in Table. They testify that the optimized value of the parameter a for the F-43m structural type differs from the experimentally measured one only by 0.18%.

As was expected, the optimized values of the parameter a for the F-43m and C1b^a modifications practically coincide. The total electron densities of states calculated for those structures are also identical (Fig. 2). Both those facts testify now that the structure modeling with the use of P lattice for the researched phases is a proper procedure.

The muffin-tin (MT) radii for the atomic spheres were chosen to minimize the dimensions of region II between the spheres in the C1b^a modification, which has the smallest volume of the unit cell. For all spatial configurations and all atoms, these radii amounted to $2.18a_0$, where $a_0 = 5.2918 \times 10^{-11}$ m is the Bohr radius. While calculating the indices of the electron band structure for all structural modifications of CoTiSb compound, 172 points were used in the irreducible part of their Brillouin zones. The APW+lo bases were used to approximate the wave functions of $3d$ electrons in all atoms, and the LAPW ones for the wave functions of other valence electrons. The product of the MT sphere radius R_{mt} and the wave vector maximum for plane waves $K_{\max}$ was chosen to equal seven. The maximum values of the quantum number were selected to equal $l = 10$ for the partial waves in the spheres and $l = 4$ in the calculation of non-muffin-tin matrix elements.

The cohesive energy was calculated as the difference between the total energy of the corresponding CoTiSb phase and the sum of the total energies of the atoms that composed that phase but moved away from each other by an "infinite" distance. The atoms were determined in accordance with the recommendations of work [13].

The polarization degree P of Fermi electrons was determined by the formula [14]

$$P = \frac{D_\uparrow(E_\mathrm{F}) - D_\downarrow(E_\mathrm{F})}{D_\uparrow(E_\mathrm{F}) + D_\downarrow(E_\mathrm{F})},$$

where $D_\uparrow(E_\mathrm{F})$ and $D_\downarrow(E_\mathrm{F})$ are the total electron densities of states at the Fermi level (E_F) with the spins directed upward and downward, respectively.

3. Discussion of the Results Obtained

As one can see from the results depicted in Fig. 3, the states with both close (with a difference of a few thousandths of electronvolt) and considerably different values of cohesive energy can be realized in the system of mentioned spatial configurations. The former expectedly include the F-43m and $C1b^a$ phases, as well as the compositions of the structural types $L2_1{}^a$ and $B2^c$. At the same time, the transition from the $C1b^a$ phase to the $L2_1{}^a$ one is accompanied by a drastic (1.024 eV) increase of the cohesive energy. As a result, the $L2_1{}^a$ and $B2^c$ phases can be regarded as metastable, energetically highly excited states, which cannot be realized in practice. The transition from the ground state into a highly excited one results in the loosening of interatomic chemical bonds, which gives rise to the growth of the parameter a, especially large at the transition into the $B2^c$ phase.

The variations in the component arrangement over the crystallographic positions of CoTiSb alloy manifest themselves in the total electron densities of states, which are shown in Fig. 4. In order to find a "true" (corresponding to the experiment) distribution of states among them, the photoelectron spectrum of CoTiSb compound [15] is also exhibited. Its c-peak is superimposed with the corresponding component in the total electron density of states obtained for the $C1b^a$ modification. This procedure of matching between the photoelectron spectra and the total electron density of states on the basis of their characteristic peaks is standard (see, e.g., works [16, 17]). A mismatch obtained between the Fermi level positions that were determined either experimentally on the scale of valence electron binding energies (E_b) or with the help of band structure calculations is caused by the fact that the excited states (a vacancy in the final state of the photoionization process) reveal themselves in the experimental case, whereas the calculation concerns the ground state of the compounds and gives underestimated values for the Fermi level energies. In our case, the indicated mismatch between the Fermi level positions amounted to 1.12 eV. As to the distributions of other electron densities in the $L2_1{}^a$ and $B2^c$ phases, they are coupled with the previous one by their Fermi levels.

From Fig. 4, it follows that the energy distribution of valence electrons corresponding to the atomic configuration of the $C1b^a$ structural type maximally correlates with the experiment. In particular, the en-

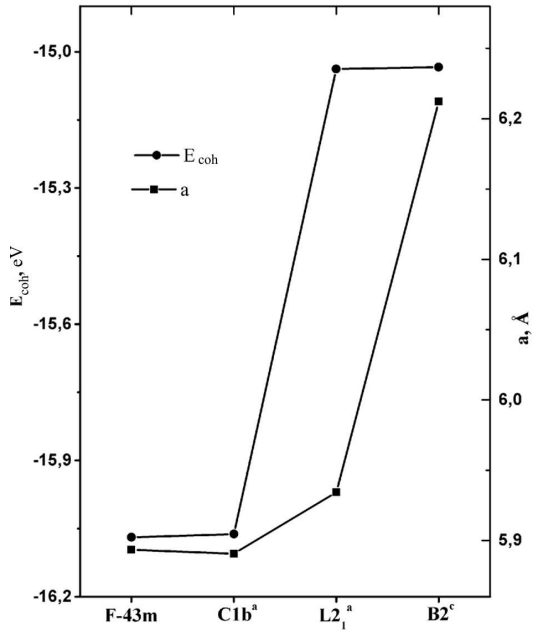

Fig. 3. Cohesive energy, $E_{\rm coh}$, and cubic cell parameter, a, for various atomic configurations of CoTiSb compound

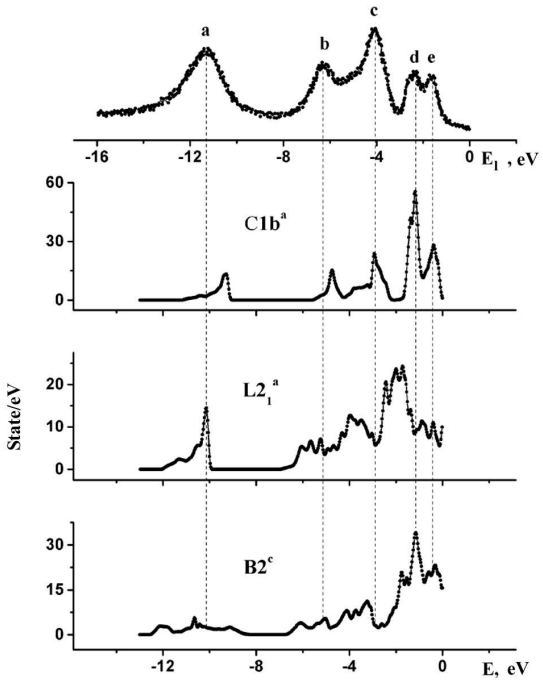

Fig. 4. Photoelectron spectrum (upper panel) of CoTiSb alloy [15] and total densities of valence electron states in its various structural modifications (indicated in the figure). Zero energy values correspond to the Fermi level position

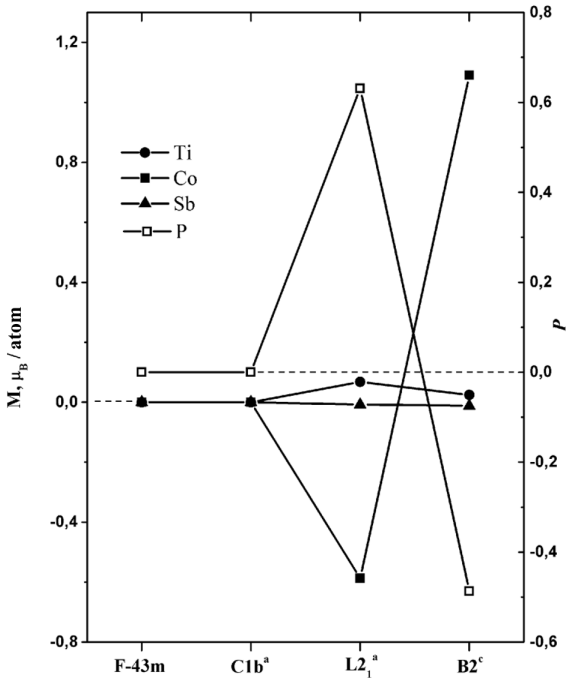

Fig. 5. Atomic magnetic moments **M** and polarization degree P of electron states in various structural modifications of CoTiSb alloy. μ_B is the Bohr magneton

ergy positions of peaks c, d, and e in the photoelectron spectrum coincide with their counterparts in the electron state distribution. At the same time, the positions of bright components a and b in the experimental spectrum correspond to humps in the density of states. The calculations also testified to a non-magnetic character (see below) of the $C1b^a$ phase. Furthermore, in this phase, there exists a direct minimum energy gap of 1.087 eV at point Γ of the Brillouin zone, which separates occupied and free electron states from one another. According to the results of other band structure calculations, the magnitude of this gap falls within an interval from 0.95 [8, 18] to 1.06 eV [15].

The revealed correlation between the calculation and experimental results testifies, first, that the proposed calculation procedure is correct; second, that the ground state of the researched compound is really realized in the atomic configuration of the $C1b^a$ structural type; and, finally, that the determination of atomic configurations in the ground state with the use of band structure calculations can be useful in the researches dealing with the spatial structure in atomically disordered compounds.

It is no surprise that the energy distributions of the total density of valence electron states for the $L2_1{}^a$ and $B2^c$ phases substantially differ from the previous one. Mismatches are observed not only in the energy positions of density components and their shapes, but also in their presence exactly at the Fermi level. Really, if the $C1b^a$ composition is an insulator with a zero density of valence electrons at the Fermi level, the other two compositions transform into metals with a state density of 9.94 state/eV for the $L2_1{}^a$ phase and 15.64 state/eV for the $B2^c$ one. Note that the overestimated value of the total density of states obtained for valence electrons at the Fermi level for the $B2^c$ phase testifies again to the extreme instability of this phase and the impossibility of its synthesis.

The transformation to metastable modifications of the examined alloy is accompanied by the spin polarization of their electron states, which is illustrated in Fig. 5. One can see that the polarization degrees P for the $L2_1{}^a$ and $B2^c$ phases substantially differ from zero. The zero polarization is typical of the ground state modifications F-43m and $C1b^a$. In turn, transitions between metastable phases change the sign of P.

The polarization of electron states substantially affects the formation of magnetic moments at the atoms in separate phases of CoTiSb alloy. From Fig. 5, it follows that the F-43m and $C1b^a$ phases of the ground state are really non-magnetic [18]. At the same time, atoms in metastable formations acquire magnetic moments. The corresponding values of magnetic moments at cobalt atoms turn out anomalously large and change their sign at the transition from a metastable phase to the other one. The variations of magnetic moments at titanium and antimony atoms are less considerable, and those moments themselves are close to zero.

4. Conclusions

The ground state of CoTiSb alloy with the largest cohesive energy is realized in the $C1b^a$ phase. Transitions to the $L2_1{}^a$ and $B2^c$ phases with different arrangements of alloy components in their crystal lattices are accompanied by the emergence of metastable high-energy excited states. CoTiSb compound is a non-magnetic insulator in the ground state, whereas the metastable phases are transformed into metals with spin-polarized electrons and the magnetic moments mainly localized at cobalt atoms.

1. R.I. Krypyakevich, V.Ya. Markiv. Crystal structures of ternary compound in the systems Ti(V)–Fe(Co, Ni)–Sn(Sb). *Dopov. Akad. Nauk UkrRSR* No. 12, 1606 (1963) (in Ukrainian).
2. T. Graf, C. Felser, S.S.P. Parkin. Simple rules for the understanding of Heusler compounds. *Prog. Solid State Chem.* **39**, 1 (2011) [DOI: 10.1016/j.progsolidstchem.2011.02.001].
3. G.E. Bacon, J.S. Plant. Chemical ordering in Heusler alloys with the general formula A_2BC or ABC. *J. Phys. F* **1**, 524 (1971) [DOI: 10.1088/0305-4608/3/11/ 020].
4. S. Ishida, T. Masaki, S. Fujii, S. Asano. Theoretical predicts of half-metallic compounds with the $C1_b$ structure. *Physica B* **239**, 163 (1997) [DOI: 10.1016/S0921-4526(97)00401-8].
5. J. Tobola, L. Jodin, P. Pecheur, G. Venturini. Unusual electron structure and electron transport properties of some disordered half-Heusler phases. *J. Alloy. Compd.* **383**, 328 (2004) [DOI: 10.1016/j.jallcom.2004.04.041].
6. P. Larson, S.D. Mahanti, M.G. Kanatzidis. Structural stability of Ni-containing half-Heusler compounds. *Phys. Rev. B* **62**, 12754 (2000) [DOI: 10.1103/PhysRevB.62.12754].
7. T. Sekimoto, K. Kurosaki, H. Muta, S. Yamanaka. Annealing effect on thermoelectric properties of TiCoSb half-Heusler compound. *J. Alloy. Compd.* **394**, 122 (2005) [DOI: 10.1016/j.jallcom.2004.11.017].
8. Y. Xia, V. Ponnambalam, S. Bhattacharya, A.L. Pope, S.J. Poon, T.M. Tritt. Electrical transport properties of TiCoSb half-Heusler phases that exhibit high resistivity. *J. Phys.: Condens. Matter* **13**, 77 (2001) [DOI: 10.1088/0953-8984/13/1/308].
9. I. Skovsen, L. Bjerg, M. Christensen, E. Nishibori, B. Balke, C. Felser, B.B. Iversen. Multi-temperature synchrotron PXRD and physical properties study of half-Heusler TiCoSb. *Dalton Trans.* **39**, 10154 (2010) [DOI: 10.1039/C0DT00742K].
10. D. Singh. *Plane Waves, Psedopotentials and LAPW Method* (Kluwer Academic, 1994).
11. J.P. Perdew, S. Burke, M. Ernzerhof. Generalized gradient approximation made simple. *Phys. Rev. Lett.* **77**, 3865 (1996) [DOI: 10.1103/PhysRevLett.77.3865].
12. P. Blaha, K. Schwarz, G.K. Madsen, D. Kvasnicka, J. Luitz. *WIEN2k, An Augmented Plane Wave + Local Orbitals Program for Calculating Crystal Properties* (Vienna Univ. of Technology, 2001) [ISBN 3-9501031-1-2].
13. http://www.wien2k.at/reg_user/faq/.
14. B.R.K. Nanda, I. Dasgupta. Electronic structure and magnetism in half-Heusler compounds. *J. Phys.: Condens. Matter* **15**, 7307 (2003) [DOI: 10.1088/0953-8984/15/43/014].
15. S. Ouardi. Ph.D. thesis *Electronic Structure and Physical Properties of Heusler Compounds for Thermoelectric and Spintronic Applications* (J. Gutenberg-Universität Mainz, 2012).
16. V.N. Uvarov, I.V. Urubkov, E.V. Urubkova, V.V. Klimov, O.Yu. Khizhun, V.V. Trachevskii. Electron structure of $NaVP_2O_7$ and $NaFeP_2O_7$ pyrophosphates: X-ray, photoelectron, NMR spectra and band structure calculations. *Metallofiz. Noveish. Tekhnol.* **33**, 145 (2011) (in Russian).
17. V.M. Uvarov, M.P. Melnyk, M.V. Uvarov, V.S. Mykhalenkov, T.L. Syzova. Electron structure of $GdMeO_3$ (Me = = V, Ni) oxides: X-ray electron, X-ray spectra and band structure calculations. *Metallofiz. Noveish. Tekhnol.* **35**, 279 (2013) (in Ukrainian).
18. J. Tobola, J. Pierre, S. Kaprzyk, R.V. Skolozdra, M.A. Kouacou. Crossover from semiconductor to magnetic metal in semi-Heusler phases as a function of valence electron concentration. *J. Phys.: Condens. Matter* **10**, 1013 (1998) [DOI: 10.1088/0953-8984/10/5/011].

Received 20.06.16.
Translated from Ukrainian by O.I. Voitenko

В.М. Уваров, М.В. Уваров,
С.А. Беспалов, М.В. Немошкаленко

АТОМНЕ РОЗУПОРЯДКУВАННЯ
ТА ЕЛЕКТРОННА БУДОВА СПЛАВУ
ХОЙСЛЕРА CoTiSb

Р е з ю м е

За допомогою лінійного методу приєднаних плоских хвиль (ЛППХ) виявлено роль деяких структурних типів сплаву CoTiSb у формуванні його енергетичних, просторових, спектральних і спінових характеристик. Встановлено, що його основний стан з найбільшим значенням когезійної енергії реалізується у разі розташування атомів і вакансій, характерного для $C1b^a$-фази. Перехід до $L2_1{}^a$-, $B2^c$-фаз з іншим положенням компонентів сплаву в його кристалічній ґратці супроводжується виникненням енергетично високозбуджених метастабільних станів. Сполука CoTiSb в основному стані є немагнітним ізолятором, метастабільні фази перетворюються на метали з спін-поляризованими електронними станами і магнітними моментами, локалізованими переважно на атомах кобальту.